# Oscillatory Magnetoresistance in Gray Tin*

E. D. HINKLEY† AND A. W. EWALD
*Department of Physics, Northwestern University, Evanston, Illinois*
(Received 10 January 1964)

The oscillatory component of magnetoresistance has been measured for single crystals of $n$-type gray tin at liquid-helium temperatures. The period of oscillation is independent of magnetic field direction, confirming an isotropic effective mass and, therefore, a conduction-band edge at the center of the Brillouin zone. Oscillations were also observed in a polycrystalline specimen. Carrier concentrations deduced from the oscillatory period are in reasonably good agreement with values obtained from the Hall coefficient over a range of almost two orders of magnitude in this parameter. An electron effective mass of 0.024 $m_0$ was obtained from the field and temperature dependence of the oscillatory amplitude for samples having carrier concentrations on the order of $10^{16}$ cm$^{-3}$. Nonthermal damping of the oscillations is attributed mainly to inhomogeneities in the impurity distribution. The experimental results are compared with theory.

## I. INTRODUCTION

In recent years oscillatory magnetoresistance measurements have provided band-structure information for several of the compound semiconductors.[1–3] The results are in agreement with those obtained from cyclotron resonance[4–6] and de Haas–van Alphen[7] experiments. Of the *elemental* semiconductors, only germanium[8] and gray tin[9] have shown an oscillatory component of the magnetoresistance. The band structure of germanium had already been established through cyclotron resonance and other measurements before the magnetoresistance oscillations were observed, and therefore, this phenomenon was not exploited. In the case of gray tin, where cyclotron resonance has not been observed, low-temperature band-structure information was lacking. Previous magnetoresistance measurements at liquid-nitrogen temperature and above had indicated a change in symmetry type from that characteristic of [111] valleys at 273°K to the spherical symmetry of a central conduction-band minimum at 77°K (see Ref. 10). The present work indicates that at lower temperatures the electrons remain in the central minimum. It also yields a value for the effective mass of electrons in this band.

This paper describes the oscillatory magnetoresistance measurements made on single crystals (and on one polycrystalline specimen) of $n$-type gray tin. The experimental data are compared with magnetoresistance theories in terms of oscillatory period, phase, and amplitude. The value of electron effective mass and the shape of the constant energy surfaces for gray tin as deduced from the data are also compared with the theoretical predictions.

## II. THEORY

When a magnetic field is applied to a system of charge carriers, the quasicontinuous distribution of states in momentum space collapses into a set of highly degenerate one-dimensional Landau subbands. Consequently, under certain conditions, the electrical resistance of a degenerate ($E_F > kT$) semiconductor is found to have an oscillatory dependence on magnetic field, periodic in reciprocal field. The oscillatory period is inversely proportional to the extremal cross-sectional area of the Fermi surface in a plane perpendicular to the magnetic field direction, and is generally a function of field orientation. For the special case of a spherical Fermi surface, however, the oscillatory period is a function only of carrier concentration.

$$P=(2e/\hbar c)(3\pi^2 n)^{-2/3}=3.18\times 10^6 n^{-2/3}, \qquad (1)$$

where $n$ is measured in cm$^{-3}$ and $P$ in reciprocal gauss.

The usual semiquantitative conditions for the occurrence of quantum oscillations require that the separation $\hbar\omega$ between Landau levels be greater than the energy spread associated with the Fermi surface electrons. There are two major causes of this energy spread: First, a thermal "fuzzing" occurs at any non-

* This is a publication of the Materials Research Center, Northwestern University. It is based on a dissertation submitted by E. D. Hinkley to the Graduate School of Northwestern University in partial fulfillment of the requirements for the degree of Doctor of Philosophy. The work was supported jointly by the U. S. Office of Naval Research and by the Advanced Research Projects Agency of the U. S. Department of Defense.

† Present address: Lincoln Laboratory, Massachusetts Institute of Technology, Lexington, Massachusetts.

[1] H. P. R. Frederikse and W. R. Hosler, Phys. Rev. **108**, 1136 (1957).

[2] R. J. Sladek, Phys. Rev. **110**, 817 (1958). H. P. R. Frederikse and W. R. Hosler, *ibid.* **110**, 880 (1958).

[3] K. F. Cuff, M. R. Ellett, and C. D. Kuglin, J. Appl. Phys. Suppl. **32**, 2179 (1961).

[4] G. Dresselhaus, A. F. Kip, C. Kittel, G. Wagoner, Phys. Rev. **98**, 556 (1955). E. Burstein, G. S. Picus, and H. A. Gebbie, *ibid.* **103**, 825 (1956).

[5] B. Lax and J. L. Mavroides, *Solid State Physics*, edited by F. Seitz and D. Turnbull (Academic Press Inc., New York, 1960), Vol. 11.

[6] U. J. Hansen and K. F. Cuff, Bull. Am. Phys. Soc. **8**, 246 (1963).

[7] P. J. Stiles, E. Burstein, and D. N. Langenberg, Bull. Am. Phys. Soc. **6**, 115 (1956).

[8] G. Lautz and W. Ruppel, Physik. Verhandl. **6**, 193 (1955). I. G. Fakidov and E. A. Zavadskii, Zh. Eksperim. i Teor. Fiz. **34**, 1036 (1958) [English transl.: Soviet Phys.—JETP **7**, 716 (1958)].

[9] E. D. Hinkley and A. W. Ewald, Bull. Am. Phys. Soc. **7**, 409 (1962). E. D. Hinkley and A. W. Ewald, Bull. Am. Phys. Soc. **8**, 245 (1963).

[10] O. N. Tufte and A. W. Ewald, Phys. Rev. **122**, 1431 (1961).

TABLE I. Gray tin sample characteristics.

| Sample | $n_H$ ($cm^{-3}$)[a] | $\sigma_{4.2}$ ($ohm^{-1}$ $cm^{-1}$) | $\sigma_{4.2}/\sigma_{1.2}$ | $\mu$ ($cm^2$/V-sec)[b] |
|---|---|---|---|---|
| A-1 | $4.17\times10^{16}$ | 772 | 1.00 | $1.16\times10^{5}$ |
| B-1[c] | $1.14\times10^{16}$ | 455 | 1.00 | $2.50\times10^{5}$ |
| B-2[c] | ... | 465 | 1.00 | ... |
| B-3 | ... | 375 | 1.00 | ... |
| B-5 | $1.28\times10^{16}$ | ... | ... | ... |
| B-6 | $0.82\times10^{16}$ | ... | ... | ... |
| B-7 | $1.76\times10^{16}$ | ... | ... | ... |
| C-1 | $4.3\times10^{15}$ | 240 | 1.04 | $3.49\times10^{5}$ |
| C-2 | $6.6\times10^{15}$ | 240 | 1.02 | $2.28\times10^{5}$ |
| D-2 | $6.4\times10^{14}$ | 63 | 4.5 | $6.2\times10^{5}$ |

[a] Obtained from Hall coefficient, $R$, at 4.2°K as $1/Re$.
[b] Calculated as the product $R\sigma$ at 4.2°K.
[c] Samples obtained from same single crystal.

zero temperature since the electrons may deviate from the Fermi surface by a few $kT$; second, collisions limit the lifetime $\tau$ of a quantum state, with concomitant uncertainty $\hbar/\tau$ in electron energy leading to the cyclotron condition $\omega\tau>1$. This condition may be written more conveniently as $\mu B>10^8$, where $\mu$ is the Hall mobility in $cm^2$/V sec and $B$ is the magnetic field in gauss.

In addition to the thermal and collision broadening of the electron energy levels described above, the Fermi level itself may vary throughout the specimen as a result of an inhomogeneous distribution of impurities. It is clear from Eq. (1) that such an effect would be manifested as a spatial variation of the oscillatory period, and partial cancellation of oscillations would occur.

The above conditions, together with their implications concerning the observation of quantum oscillations at readily obtained steady magnetic fields, are summarized below:

(1) $\hbar\omega>kT$. Low carrier effective mass, low ambient temperature.
(2) $\mu B>10^8$. High carrier mobility.
(3) $\hbar\omega>\Delta E_F$. Homogeneous specimen.

A recent theory for transverse ($B\perp I$) oscillatory magnetoresistance proposed by Adams and Holstein[11] embodies all the above conditions, except for inhomogeneity broadening. The latter is taken into account by defining a combined nonthermal broadening temperature $T'$ as the sum of the collision (Dingle) and inhomogeneity broadening temperatures. The analysis of Adams and Holstein, while limited to materials with spherical Fermi surfaces, shows the oscillatory phenomenon to be essentially independent of the type of scattering. On the basis of their derivation, the oscillatory part of the transverse magnetoresistance of interest here may be written as

$$\frac{\Delta\rho_{0sc}}{\rho_0}=5\sqrt{2}\pi^2\frac{kT}{E_F^{1/2}(\hbar\omega)^{1/2}}\sum_{M=1}^{\infty}\frac{M^{1/2}(-1)^M e^{-2\pi^2M(kT'/\hbar\omega)}}{\sinh[2\pi^2M(kT/\hbar\omega)]}\times\cos\left[\frac{2\pi ME_F}{\hbar\omega}-\frac{\pi}{4}\right], \quad (2)$$

where $\rho_0$ is the zero-field resistivity and $M$ is the harmonic of the oscillations. This expression may be simplified because only the fundamental ($M=1$) is usually significant. In addition, the hyperbolic sine may be replaced by its exponential approximation. Equation (2) then reduces to

$$\frac{\Delta\rho_{0sc}}{\rho_0}=-10\sqrt{2}\pi^2\frac{kT}{E_F^{1/2}(\hbar\omega)^{1/2}}\times\exp\left[-\left(\frac{2\pi^2k}{\beta_0}\right)\left(\frac{m^*}{m_0}\right)\left(\frac{T+T'}{B}\right)\right]\cos\left(\frac{2\pi}{PB}-\frac{\pi}{4}\right), \quad (3)$$

where the oscillatory period $P$, the effective mass $m^*$, and $\beta_0(=e\hbar/m_0c$, the double Bohr magneton) have been introduced.

Oscillations in the longitudinal ($B||I$) magnetoresistance have been treated by Argyres.[12] The corresponding equation is identical with Eq. (3) when the latter is reduced by a factor of 5.

## III. EXPERIMENTAL DETAILS

### A. Specimens

Gray tin crystals were grown from mercury solution by the procedure of Ewald and Tufte.[13] Crystals of various impurity concentrations were available as a result of different purification processes carried out on the commercial zone-refined tin. The different purities were reflected in different carrier concentrations at 4.2°K as determined by the Hall coefficient. The samples ranged in carrier concentration from $6.4\times10^{14}$ $cm^{-3}$ to $4.2\times10^{16}$ $cm^{-3}$ and on this basis were divided into four categories designated by a letter prefix to the sample number as shown in Table I. The donor impurity atoms are probably antimony which is not removed during the zone-refining process, and only partially removed during subsequent purification. Cutting of the crystals into rectangular parallelepipeds suitable for electrical measurements was performed with a sand-blast unit. Sample dimensions were approximately $0.2\times0.4\times3$ mm.

Samples were mounted on Bakelite holders at the end of long, thin-walled Monel tubes. Current electrodes, which also served as support for the sample, were of No. 36 copper wire and were attached to the ends of the

[11] E. N. Adams and T. D. Holstein, Phys. Chem. Solids **10**, 254 (1959).

[12] P. N. Argyres, Phys. Chem. Solids **4**, 19 (1958).
[13] A. W. Ewald and O. N. Tufte, J. Appl. Phys. **29**, 1007 (1958)

sample with gallium-indium (3 parts Ga to 1 part In) solder. To reduce adverse effects due to large area potential-probe contacts, the following soldering procedure was employed. Bare No. 56 (0.0127 mm) copper wires, which served as the potential probes, were first "tinned" and then brought into contact with the cooled sample at the desired locations. A 200 mA current pulse was then passed through the potential leads producing localized heating which melted the solder. By this means the solder contact area was held to less than that of the wires. The potential probes were usually attached to the side of the sample and (to eliminate "edge" effects) at a distance from the ends greater than the sample width. In some instances, however, the potential probes were mounted at the ends of the specimens with the current electrodes.

### B. Apparatus and Procedure

The sample was immersed directly in liquid helium. Temperatures below 4.2°K were obtained by pumping on the helium vapor, and were measured by the vapor pressure. The lower tip of the helium Dewar was located between the pole pieces of a magnet which could be rotated in the horizontal plane. Magnet current was supplied by a bank of storage batteries, and regulated by water-cooled rheostats.

A constant current of up to 10 mA was supplied to the sample by a high-impedance transistorized current source. Maximum sample current was determined by the condition that the rise in sample temperature as a result of joule heating should not be excessive. Analysis of the oscillatory amplitudes for a sample under varying conditions of power dissipation showed that if the input power was less than 100 $\mu$W, sample temperature rose by less than 0.1°K.

The amplified voltage from the potential probes was applied to the $Y$ axis of an $X$-$Y$ recorder, the $X$ axis of which was driven by a signal proportional to the current through the magnet. Magnetic field values corresponding to various positions along the $X$ axis were obtained from a calibration curve made with a rotating-coil fluxmeter. In those cases in which the nonoscillatory part of the magnetoresistance was approximately linear with field, a bucking voltage proportional to magnet current was used to permit greater amplification of the oscillations. For precise measurements, e.g., to determine Hall voltage or zero-field resistance, the electrometer amplifier was replaced by a potentiometer.

## IV. DATA REDUCTION TECHNIQUE

### A. Oscillatory Period and Phase

The period and phase of the magnetoresistance oscillations were usually obtained from a direct analysis of the $X$-$Y$ recorder curves. (In order to determine the nonoscillatory magnetoresistance, however, the data had to be averaged over positive and negative field directions to cancel Hall voltage contributions resulting from misalignment of the potential probes.) Envelope curves were constructed tangent to the oscillations with a nodal line drawn halfway between. The intersections of the nodal line with the recorder curve located the nodes of the oscillations which were used to determine the period and phase.

Equation (3) may be expressed in terms of an amplitude $A$, period $P$, and phase $\phi$ as

$$\Delta\rho_{0sc}/\rho_0 = A(B,T)\cos[(2\pi/PB+\phi+\pi], \quad (4)$$

where the minus sign has been absorbed into the argument of the cosine. A node occurs whenever the argument of the cosine is an odd integer multiple of $\pi/2$. This condition may be stated as

$$(2\pi/PB_n)+\phi+\pi=(2n+\tfrac{1}{2})\pi, \quad (5)$$

where $n$ takes on both integer and half-integer values corresponding to the two nodes per oscillation. Ambiguity in the assignment of integers and half-integers to the experimentally observed nodes is removed by noting that, according to Eqs. (4) and (5), the oscillatory curve (as a function of $B$) has positive slope at the integer nodes and negative slope at the half-integer nodes. This point is very important to an experimental determination of phase. A plot of reciprocal magnetic field values at which the nodes occur versus integers and half-integers represents a straight line of slope $P$. The intercept $n_0$ with the $1/B=0$ axis is related to the phase. These relationships become clear upon rearranging Eq. (5) into the following form:

$$1/B_n = Pn-[(\phi/2\pi)+\tfrac{1}{4}]P. \quad (6)$$

The phase can be deduced from $n_0$ by the expression

$$\phi=(2n_0-\tfrac{1}{2})\pi. \quad (7)$$

If the measured phase agrees with the predicted value of $-\frac{1}{4}\pi$, then $n_0=\frac{1}{8}$. For future reference, an intercept $n_0=0$ implies a phase of $-\frac{1}{2}\pi$. Since integral multiples of $2\pi$ may be added algebraically to $\phi$ without altering the situation, $n_0$ is likewise arbitrarily defined with respect to the integers.

### B. Effective Mass

Equation (1) shows that, for a semiconductor having spherical constant-energy surfaces, the oscillatory period is a function only of carrier concentration, and is, therefore, independent of the effective mass. The effective mass parameter is, however, contained in the oscillatory amplitude expression,

$$A(B,T)\propto B^{-1/2}\exp[-\gamma(m^*/m_0)(T+T')/B], \quad (8)$$

where $\gamma\equiv 2\pi^2k/\beta_0=14.68\times10^4$ gauss/deg If the above equation is multiplied by $B^{1/2}$, and the logarithm of the resulting expression differentiated with respect to $1/B$,

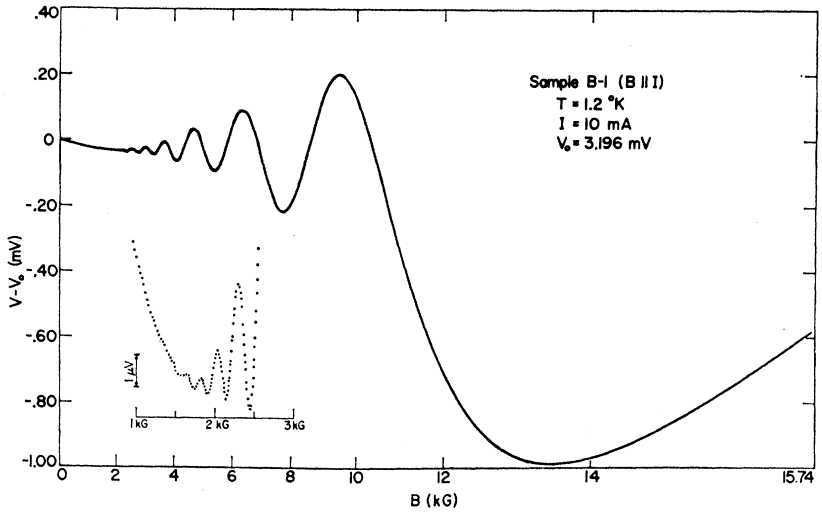


FIG. 1. Recorder traces of magnetoresistance voltage versus magnet current for gray tin single-crystal sample B-1 at 1.2°K. Data in the low-field region (inset) were recorded point-by-point because the signal was comparable to induced voltages occurring when the magnetic field was changed. Magnetic field is parallel to sample current.

the following is obtained:

$$d\ln(AB^{1/2})/d(1/B) = -\gamma(m^*/m_0)(T+T'). \quad (9)$$

Therefore, a logarithmic plot of $AB^{1/2}$ versus $1/B$ yields a straight line, the slope of which is proportional to the product $m^*(T+T')$. The unknown quantities $m^*$ and $T'$ may be evaluated by analyzing the field dependence of the oscillatory amplitude for at least two different ambient temperatures. For some of the samples tested *several* ambient temperatures were used in an attempt to overdetermine the effective mass value and (hopefully) increase its accuracy. We found it convenient to define a slope function $S(T)$ equal to the negative of Eq. (9). The points of an $S$ versus $T$ plot represent a straight line having slope $\gamma(m^*/m_0)$ and an intercept (at the $T=0$ axis) of $\gamma(m^*/m_0)T'$.

## V. RESULTS AND DISCUSSION

### A. Oscillatory Parameters

Figure 1 shows actual recorder traces of voltage across the potential probes of sample B-1 as a function of magnet current. The continuous curve exhibits oscillations starting somewhat above 2 kG. Oscillations at still lower fields are apparent in the inset curve which was taken with one hundred times greater amplification. The latter curve was recorded point-by-point to eliminate traces of induced voltages due to the quasi-continuous change in magnetic field.

Since sample B-1 exhibited the largest number of detectable oscillations of all those tested, it was of special interest to our investigation. Figures 2 and 3 show the transverse and longitudinal magnetoresistance field dependences, respectively, for this sample. It is noteworthy that the oscillatory amplitudes for the two modes are approximately the same, although an order of magnitude smaller than predicted by Eq. (3). The nonoscillatory magnetoresistance components differ

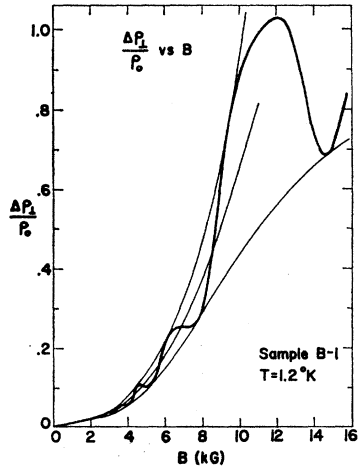


FIG. 2. Field dependence of transverse magnetoresistance for sample B-1 at 1.2°K. This curve was obtained by averaging data for positive and negative field directions. A line of nodes has been constructed midway between envelope lines, and was used to determine the oscillatory period and phase.

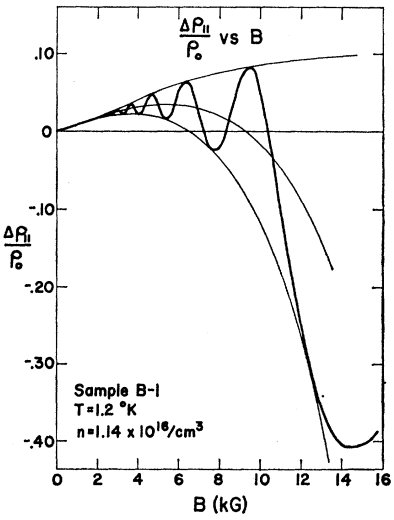


FIG. 3. Field dependence of longitudinal magnetoresistance for sample B-1 at 1.2°K. Negative longitudinal magnetoresistance was observed for all samples in the high-field region.

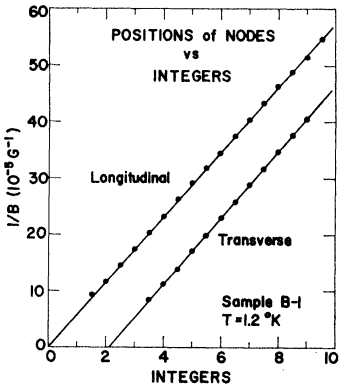


FIG. 4. Nodal positions of transverse and longitudinal magnetoresistance oscillations for sample B-1 are plotted versus integers and half-integers. The oscillatory periods and phases were obtained from the slopes and intercepts, respectively, of the straight lines.

markedly between the transverse and longitudinal modes, and the *negative* longitudinal magnetoresistance apparent at high fields was observed at liquid-helium temperatures for all samples. Node-integer plots for both orientations of magnetic field are shown in Fig. 4. The oscillatory periods deduced from the slopes in accordance with Eq. (6) are $5.84\times10^{-5}$ $G^{-1}$ for the transverse mode and $5.72\times10^{-5}$ $G^{-1}$ for the longitudinal mode. Since this sample was mounted so that the magnetic field for both modes was [110] oriented, this agreement is expected.

A detailed study of the dependence of oscillatory period on crystal orientation was made using sample B-6. Figure 5 shows the oscillatory period for this sample as a function of magnetic field direction. If we attribute the 3% scatter of points to errors in the data reduction, we conclude that the period is independent of crystal orientation. This *indifference* of oscillatory period to magnetic field direction relative to the crystal axes was found on all samples and is the basis for concluding that, at liquid helium temperatures, the electrons occupy a spherically symmetric band.

The absence of a crystal orientation dependence of the oscillatory period was also verified by the method

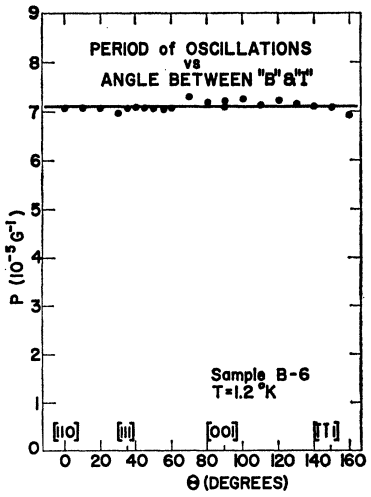


FIG. 5. Angular dependence of oscillatory period for sample B-6. Sample current is in the [110] direction, with magnetic field in the (1$\bar{1}$0) plane. The 3% scatter of points from the average value is attributed to errors in the graphical data reduction procedure.

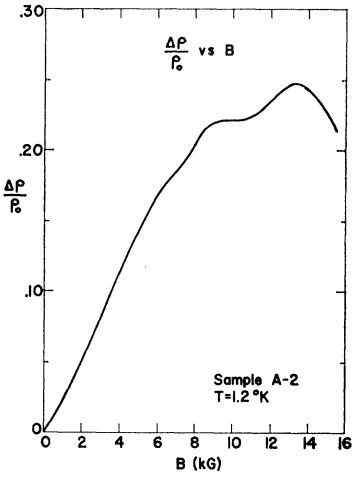


FIG. 6. Field dependence of magnetoresistance for polycrystalline sample A-2. The presence of oscillations confirms the orientation-independence of oscillatory period.

of Sladek[2] which utilizes a polycrystalline specimen. A sample was prepared by transforming a thin white-tin foil to the gray phase. (X-ray analysis has shown that samples prepared in this manner are highly polycrystalline.) The magnetoresistance field dependence for this

TABLE II. Results of oscillatory analysis.

| Sample | $n_H$ (cm$^{-3}$) | $n_P$ (cm$^{-3}$) | $m^*/m_0$ | $T'$ (°K)[a] |
|---|---|---|---|---|
| A-1 | $4.17\times10^{16}$ | $2.16\times10^{16}$ | ... | ... |
| B-1[b] | $1.14\times10^{16}$ | $1.30\times10^{16}$ | 0.024[c] | 3.2 |
| B-2[b] | ... | $1.45\times10^{16}$ | 0.025 | 5.4 |
| B-3 | ... | $1.07\times10^{16}$ | 0.021 | 9.3 |
| B-5 | $1.28\times10^{16}$ | $0.97\times10^{16}$ | 0.023[c] | 5.3 |
| B-6 | $0.82\times10^{16}$ | $0.96\times10^{16}$ | 0.022 | 5.4 |
| B-7 | $1.76\times10^{16}$ | $1.28\times10^{16}$ | ... | ... |
| C-1 | $4.3\times10^{15}$ | $4.2\times10^{15}$ | 0.025[c] | 3.9 |
| C-2 | $6.6\times10^{15}$ | $5.0\times10^{15}$ | ... | ... |
| D-2 | $6.4\times10^{14}$ | $5.7\times10^{14}$ | ... | ... |

[a] Combined nonthermal broadening temperature.
[b] Samples obtained from same single crystal.
[c] Effective mass value determined on the basis of seven different ambient temperatures. Others on basis of two different ambient temperatures.

sample is shown in Fig. 6, where the presence of oscillations confirms sphericity of the constant energy surfaces.

Equation (1) may now be used to compare the carrier concentration $n_P$ as measured by the oscillatory period,

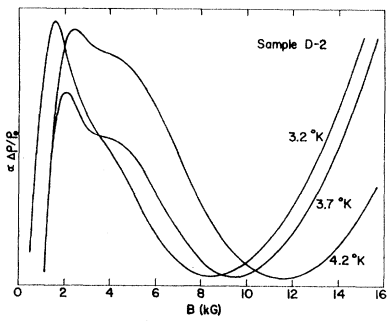


FIG. 7. Field dependence of magnetoresistance for pure sample D-2. The increase of oscillatory period with a decrease in temperature is caused by carrier freeze-out.

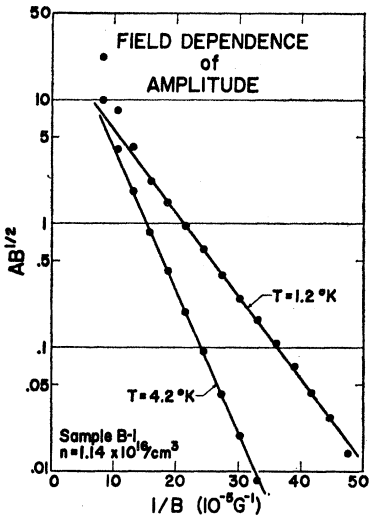


FIG. 8. Field dependence of oscillatory amplitude for sample B-1 at ambient temperatures of 4.2 and 1.2°K. Slopes are proportional to the product $m^*(T+T')$.

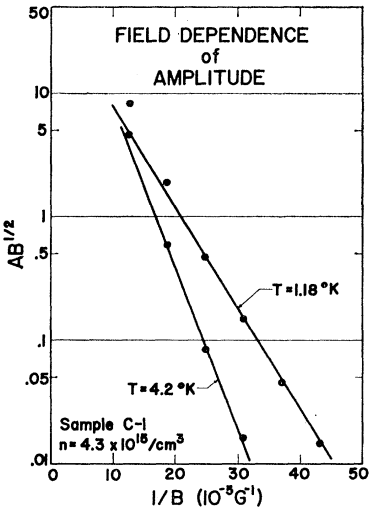


FIG. 10. Field dependence of oscillatory amplitude for sample C-1 at ambient temperatures of 4.2 and 1.18°K. Smaller number of data points (cf. Fig. 8) reflects longer period of this higher purity specimen.

with that given by the Hall coefficient. For sample B-1, $n_P=1.30\times10^{16}$ cm$^{-3}$, whereas $n_H=1.14\times10^{16}$ cm$^{-3}$. Similar comparisons for other samples are shown in Table II. It should be noted that the $n_H$ value for any particular sample is probably somewhat dependent on the location of the Hall probes because of inhomogeneity in the impurity distribution.

Small magnetoresistance oscillations were detected in the very pure sample D-2 at 4.2°K. The large decrease in conductivity for this sample from 4.2 to 1.2°K (cf. Table I) led to a search for a temperature dependence of the oscillatory period, indicative of carrier freeze-out. Figure 7 illustrates the magnetoresistance field dependence for sample D-2 at three different ambient temperatures. The period is very long (corresponding to a carrier concentration of only $6.4\times10^{14}$ cm$^{-3}$), but a change of period with temperature is quite apparent. A shifting of the extrema toward smaller magnetic field values with decreasing temperature indicates an increasing period, in qualitative agreement with Eq. (1).

For a discussion of oscillatory phase, we return to Fig. 4. The intercepts $n_0$ for the transverse and longitudinal modes are $\frac{1}{8}$ and 0, respectively, which correspond to phases of $-\frac{1}{4}\pi$ and $-\frac{1}{2}\pi$. Thus, the measured *transverse* phase agrees with theory, but a significant discrepancy exists for the *longitudinal* mode (predicted to be $-\frac{1}{4}\pi$ also). Several further measurements were made on this particular sample over a period of a few months (between which the sample was removed from its holder), and the above phases were consistently obtained. Moreover, a transverse phase of $-\frac{1}{4}\pi$ was observed on all other samples as well.

### B. Electron Effective Mass Determination

The magnetic field dependence of the oscillatory amplitudes for sample B-1 at ambient temperatures of 1.2 and 4.2°K is shown in Fig. 8. [Deviations from linearity at the high-field region stem, at least in part, from a breakdown of the hyperbolic sine approximation

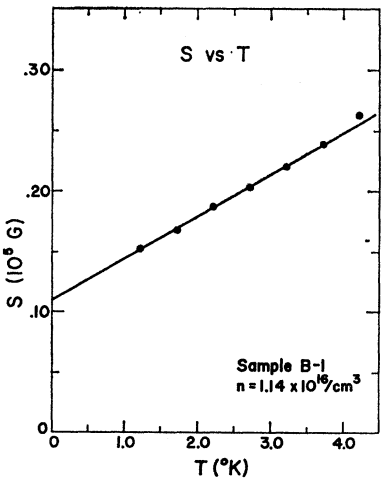


FIG. 9. Temperature dependence of slope function for sample B-1. Slope of line through points equals $\gamma(m^*/m_0)$. Intercept with ordinate equals $\gamma(m^*/m_0)T'$.

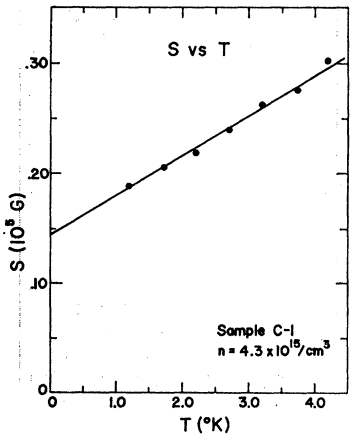


FIG. 11. Temperature dependence of slope function for sample C-1.

of Eq. (3).] Five other intermediate temperatures at half-degree intervals were also used, but these data were omitted for clarity. In Fig. 9 are shown the slopes $S(T)$ for all seven ambient temperatures. From the slope and intercept of this straight line an effective mass value of $0.024m_0$ was found, together with a combined nonthermal broadening temperature, $T'$, of 3.2°K.

A similar procedure was followed for sample C-1, with the results shown in Figs. 10 and 11. Because of the fewer detectable oscillations exhibited by this higher purity sample, the results are somewhat less accurate, as is evidenced by the larger spread of points in Fig. 11. Nevertheless, an effective mass value of $0.025m_0$ was found, with $T'=3.9$°K.

In Table II are listed the experimentally obtained values for the electron effective mass in gray tin. Although $T'$ varies from 3.2° to 9.3°K, the mass values themselves are fairly consistent. As mentioned previously, $T'$ is the sum of the Dingle and inhomogeneity broadening temperatures. Because of the high mobility of these specimens, the Dingle temperature is less than 1°K (cf. Ref. 2). Consequently, we conclude that the major contribution to $T'$ is from inhomogeneities in the specimens.

The spherical symmetry of the conduction band observed experimentally and discussed in the previous section was predicted by Herman,[14] and Liu and Bassani.[15] However, the calculated effective mass value of $0.0036m_0$ (see Ref. 16) which is based in part on the experimental band gap, is almost an order of magnitude smaller than our most accurate value of $0.024m_0$. Correction of the experimental value for nonparabolicity of the band[17] reduces it only slightly, to $0.020m_0$. To account for the relatively large observed mass as well as the pressure behavior of the conductivity at temperatures below 160°K, Groves and Paul[18] have recently proposed a new model for the band structure of gray tin. In this the direct gap is fixed at zero at all temperatures, and the temperature dependence of the conductivity in the intrinsic range is attributed to transitions from the uppermost valence band edge to [111] valleys. While a detailed quantitative comparison between the predictions of this model and all experimental data has not yet been made, the model appears to be more successful than the usual nonzero gap model in accounting for the experimental results in the lower temperature range.

## VI. CONCLUSION

An oscillatory component of magnetoresistance has been observed at liquid-helium temperatures in single crystals of $n$-type gray tin. Exceptions to the general agreement between the experimental results and the theories of Adams and Holstein, and Argyres are the smaller observed amplitude and a measured longitudinal phase of $-\frac{1}{2}\pi$.

The *indifference* of oscillatory period to magnetic-field orientation relative to the crystal axes indicates that the minimum of the conduction band is at the center of the Brillouin zone, in agreement with the theoretical predictions of Herman, and Liu and Bassani. This was also confirmed by detecting oscillations in a polycrystalline specimen. A dependence of the oscillatory period on temperature observed in a very pure specimen was attributed to carrier freeze-out.

On the basis of the field and temperature dependence of the oscillatory amplitude we have obtained an electron effective mass value of $0.024m_0$, which does not appear to depend on carrier concentration. This is much larger than the value $0.0036m_0$ calculated by Bassani and Liu, and suggests that a major revision of the band structure model, such as that recently proposed by Groves and Paul, is required.

[14] F. Herman, J. Electron. **1**, 103 (1955).

[15] L. Liu and F. Bassani, Bull. Am. Phys. Soc. **8**, 51 (1963).

[16] F. Bassani and L. Liu, Phys. Rev. **132**, 2047 (1963).

[17] J. Kolodziejczak, *Proceedings of the International Conference on Semiconductor Physics, Prague, 1960* (Academic Press Inc., New York, 1961), p. 950.

[18] Steven Groves and William Paul, Phys. Rev. Letters **11**, 194 (1963).